AIM electron density analysis on the structure and bonding in oxiranes

ARTICLE *in* JOURNAL OF MOLECULAR STRUCTURE THEOCHEM · JUNE 2002

Impact Factor: 1.37 · DOI: 10.1016/S0166-1280(02)00061-1

2 AUTHORS, INCLUDING:

Ricardo Mosquera
University of Vigo
144 PUBLICATIONS **1,814** CITATIONS

SEE PROFILE

ELSEVIER

Journal of Molecular Structure (Theochem) 586 (2002) 47–56

THEO CHEM

www.elsevier.com/locate/theochem

AIM electron density analysis on the structure and bonding in oxiranes

Antonio Vila[a], Ricardo A. Mosquera[b,*]

[a]*Departamento de Física Aplicada, Facultade de Ciencias do Campus de Ourense, Universidade de Vigo, 32004 Ourense, Galicia, Spain*
[b]*Departamento de Química Física, Facultade de Ciencias do Campus de Vigo, Universidade de Vigo, 36200 Vigo, Galicia, Spain*

Received 4 December 2001; revised 29 January 2002; accepted 29 January 2002

Abstract

The atoms in molecules (AIM) approach has been employed to characterise the structures and bonding of methyl-substituted oxiranes on B3LYP/6-311++G(d,p) electron distributions. The COC ring appeared to be a rather rigid structure upon methyl substitution, only a slight stretching of the cyclic bonds was observed. The lack of correlation between the charge density and the length of the bond path for the C–C bonds can be accounted for in terms of the electron delocalisation over the entire surface of the ring. Ring opening upon protonation was analysed and the employment of the total energy density at the bond critical point was confirmed to be a useful gauge of bonding. Closed-shell interactions were encountered between hydrogen atoms connected to carbon atoms in 1,4-positions. Regarding the transferability of non-energetic atomic and bond properties, oxygen atoms in alkyl-substituted oxiranes can be classified into two groups according to the homologous linear (branched or unbranched) monoether that would be produced by a hypothetical hydrogenation of the C–C cyclic bond. Their evolution within each series can be rationalised by considering the same six groups previously described in linear unbranched ethers.

Keywords: Atoms in molecules theory; Oxiranes; DFT calculations; Transferability; Protonation

1. Introduction

Oxirane and its derivatives play a pivotal role as organic reagents [1]. Also, in a computational sense, oxirane has been considered as a prototype of heterocycle to test the performance of new theoretical methodologies. Thus, theoretical calculations on both neutral [2–8] and protonated [2,3,9–12] oxirane can be found in the literature. The possible ring opening upon protonation in oxirane has also been described elsewhere [13–16]. Nonetheless, there is little work on methyl-substituted oxiranes. Our literature search indicates that calculations have only been reported on methyl-oxirane [6] and 1,1-dimethyloxirane [3]. This prompted us to carry out theoretical calculations on the complete set of methyl-substituted oxiranes and their protonated forms.

This work continues our extensive research into the topological properties of alkyl ethers. Our previous papers focussed on the transferability in linear monoethers [17,18] and diethers [19], protonation of monoethers [20], and the evaluation of strain energy in small ring ethers [2]. According to the results obtained in these studies, we have proposed that six different oxygen atoms should be distinguished along the linear alkyl ethers series. As an example, the properties of the oxygen in dimethylether are substantially

* Corresponding author. Fax: +34-986-8123-82.
E-mail address: mosquera@uvigo.es (R.A. Mosquera).

0166-1280/02/$ - see front matter
PII: S0166-1280(02)00061-1

Table 1
Nomenclature and energies of the alkyl-substituted oxiranes under consideration

	R1	R2	R3	R4	E (a.u.)
1	H	H	H	H	−153.83069
1 +					−154.13907
2	Me	H	H	H	−193.16849
2 + (a)					−193.48322
2 + (b)					−193.48276
3	Me	Me	H	H	−232.49917
3 +					−232.82416
4	Me	H	H	Me	−232.50068
4 +					−232.82497
5	Me	H	Me	H	−232.49859
5 + (a)					−232.82329
5 + (b)					−232.82243
6	Me	Me	Me	H	−271.82902
6 + (a)					−272.16188
6 + (b)					−272.16144
7	Me	Me	Me	Me	−311.15519
7 +					−311.49410
8	Et	H	H	H	−232.49268
9	Et	H	H	Me	−271.82484
10	Et	H	H	Et	−311.14926
11	Pr	H	H	Me	−311.14913
12	Pr	H	H	H	−271.81701
13	Pr	H	H	Et	−350.47359
14	Pr	H	H	Pr	−389.79797

For definitions of (a) and (b) see Section 3.

modified when the linear alkyl chain is increased. One of the objectives of this work is to investigate if an oxygen atom included in such a specific environment as a strained cycle does also display this kind of behaviour. This will be accomplished by analysing the DFT structural parameters together with the electron density topological indices as obtained within the atoms in molecules theory (AIM) [21,22] formalism. A related work, devoted to study the origin of the strain energy, deals with the analysis of integrated atomic properties and protonation energies in these compounds [23].

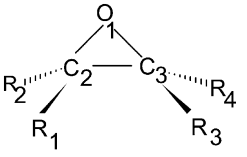

Fig. 1. Nomenclature and arrangement of the methyl-substituted oxiranes studied in this work.

2. AIM theory and computational procedure

The theory of atoms in molecules, developed by Prof. Bader's research group [21,22] leads to a quantum-mechanical rigorous partitioning of a molecule into its constituent atoms. According to AIM, the atomic basins lie within all zero-flux surfaces that surround the nucleus. Atomic properties like electron population, $N(\Omega)$, or total energy, $E(\Omega)$, can thus be obtained by integration of the proper density function within the atomic basin. The vanishing of $L(\Omega)$ (this quantity is proportional to the atomic integral of the Laplacian of the charge density) has also been employed to test the accuracy within the interatomic surfaces have been determined.

The AIM theory also recovers the main elements of molecular structure, in terms of the critical points of the charge density. Two of them are of interest: (i) the bond critical point, BCP, located approximately in between the nuclei of two bonded atoms; and (ii) the ring critical point, RCP, which appears as a consequence of any ring of bonded atoms. The two gradient paths linking the BCP with the two bonded nuclei define an atomic interaction line (AIL). We characterise the BCPs and RCPs according to the local properties: electronic charge density, ρ; Laplacian of the charge density, $\nabla^2\rho$; and total energy density [24], H. From now onward, local properties at BCP and RCP are indicated by the subscripts b and r, respectively. Also of interest at the BCP is bond ellipticity, defined as $\varepsilon = (\lambda_1/\lambda_2 - 1)$ where λ_1 and λ_2 are the largest and smallest of the two curvatures of the charge density perpendicular to the bond path, respectively.

DFT/B3LYP calculations on 14 neutral oxiranes (Table 1, Fig. 1) and the protonated forms of seven of them were carried with the GAUSSIAN 94 program [25]. For compounds with Et or Pr groups, the conformers with antiperiplanar disposition for the O–C–C–C units were the only ones considered. The geometries were fully optimised and the harmonic vibrational frequencies were also calculated at the B3LYP/6-311++G(d,p) level. The evaluation of local properties was performed using MORPHY98 [26,27] and numerical integrations were carried out using the AIMPAC program series [28,29] on B3LYP/6-311++G(d,p) electron densities.

Table 2
Selected geometrical parameters for the different neutral and protonated methyl-substituted oxiranes. Values in brackets indicate the AIL length minus geometrical bond length and the corresponding difference in bond angle. Distances in angstroms and angles in degrees

Complex	R_{C2-O1}[a]	R_{C3-O2}	R_{C3-C2}	$\alpha_{C3-O1-C2}$[a]
1	1.431 (0.002)	1.431 (0.002)	1.467 (0.015)	61.7 (12.2)
2	1.436 (0.002)	1.434 (0.002)	1.468 (0.016)	61.5 (12.1)
3	1.444 (0.002)	1.435 (0.002)	1.471 (0.017)	61.5 (12.2)
4	1.439 (0.002)	1.439 (0.002)	1.470 (0.017)	61.4 (11.6)
5	1.439 (0.002)	1.439 (0.002)	1.477 (0.017)	61.2 (12.2)
6	1.447 (0.002)	1.440 (0.002)	1.477 (0.017)	61.6 (12.3)
7	1.447 (0.002)	1.447 (0.002)	1.488 (0.018)	61.9 (12.7)
1 +	1.528 (0.069)	1.528 (0.069)	1.460 (0.013)	57.1 (5.7)
2 + (a)	1.601 ( )	1.511 (0.061)	1.463 (0.023)	55.9 ( )
2 + (b)	1.589 (0.163)	1.515 (0.037)	1.463 (0.013)	56.1 (1.1)
3 +	1.787 ( )	1.479 (0.011)	1.469 (0.017)	52.4 ( )
4 +	1.573 (0.084)	1.562 (0.070)	1.466 (0.012)	55.7 (4.7)
5 + (a)	1.569 (0.074)	1.569 (0.074)	1.471 (0.012)	55.9 (5.3)
5 + (b)	1.566 (0.078)	1.566 (0.078)	1.467 (0.023)	55.9 (5.3)
6 + (a)	1.649 ( )	1.538 (0.054)	1.475 (0.021)	54.9 ( )
6 + (b)	1.666 ( )	1.533 (0.047)	1.475 (0.021)	54.8 ( )
7 +	1.598 (0.070)	1.598 (0.070)	1.487 (0.011)	55.4 (5.4)

[a] Empty brackets represent the lack of an AIL in the protonated compound that impedes the calculation of the corresponding length or angle.

3. Structures and bonding

Table 1 presents the molecular energies of the neutral and protonated compounds under investigation. The optimised structures are local minima on the potential energy surface, all frequencies being real. In cases of two possible asymmetric oxygen protonations, the labels (a) and (b) indicate that the proton is at the same (b) or opposite (a) side of the C2–O1–C3 plane that the substituents R1 and R3

Table 3
Local properties (a.u.) at bond peripheral critical points

	C2–O1				C3–O1				C3–C2			
	ρ_b	$\nabla^2\rho_b$	H_b	ε	ρ_b	$\nabla^2\rho_b$	H_b	ε	ρ_b	$\nabla^2\rho_b$	H_b	ε
1	0.2489	−0.3581	−0.3043	0.620	0.2489	−0.3581	−0.3042	0.6196	0.2554	−0.5584	−0.2288	0.241
2	0.2466	−0.3519	−0.2973	0.627	0.2471	−0.3543	−0.2986	0.6372	0.2569	−0.5660	−0.2302	0.229
3	0.2434	−0.3444	−0.2870	0.635	0.2469	−0.3576	−0.2972	0.6199	0.2569	−0.5656	−0.2293	0.221
4	0.2449	−0.3478	−0.2916	0.638	0.2449	−0.3476	−0.2914	0.6391	0.2582	−0.5714	−0.2310	0.218
5	0.2450	−0.3527	−0.2923	0.607	0.2451	−0.3529	−0.2925	0.6670	0.2553	−0.5555	−0.2260	0.223
6	0.2418	−0.3443	−0.2819	0.614	0.2449	−0.3559	−0.2910	0.5869	0.2551	−0.5532	−0.2247	0.215
7	0.2419	−0.3555	−0.2818	0.552	0.2419	−0.3559	−0.2821	0.5514	0.2504	−0.5268	−0.2156	0.215
1 +	0.1899	−0.0026	−0.1647	1.379	0.1899	−0.0025	−0.1647	1.3794	0.2738	−0.7047	−0.2541	0.025
2 + (a)					0.1977	−0.1031	−0.1913	0.8365	0.2754	−0.7139	−0.2547	0.016
2 + (b)	0.1693	0.1995	−0.1012	5.336	0.1961	−0.0884	−0.1878	0.9014	0.2753	−0.7124	−0.2548	0.021
3 +					0.2158	−0.2607	−0.2454	0.3441	0.2765	−0.7254	−0.2529	0.007
4 +	0.1742	0.0766	−0.1256	1.643	0.1780	0.0389	−0.1368	1.3526	0.2759	−0.7132	−0.2491	0.018
5 + (a)	0.1750	0.0576	−0.1301	1.447	0.1750	0.0577	−0.1298	1.4466	0.2730	−0.6979	−0.2491	0.016
5 + (b)	0.1766	0.0458	−0.1365	1.401	0.1766	0.0457	−0.1287	1.4010	0.2723	−0.6958	−0.2473	0.023
6 + (a)					0.1874	0.0803	−0.1674	0.7387	0.2732	−0.6975	−0.2474	0.012
6 + (b)					0.1900	−0.1023	−0.1669	0.6759	0.2730	−0.6958	−0.2472	0.015
7 +	0.1649	0.0831	−0.1109	1.340	0.1650	0.0817	−0.1114	1.3595	0.2675	−0.6624	−0.2365	0.014

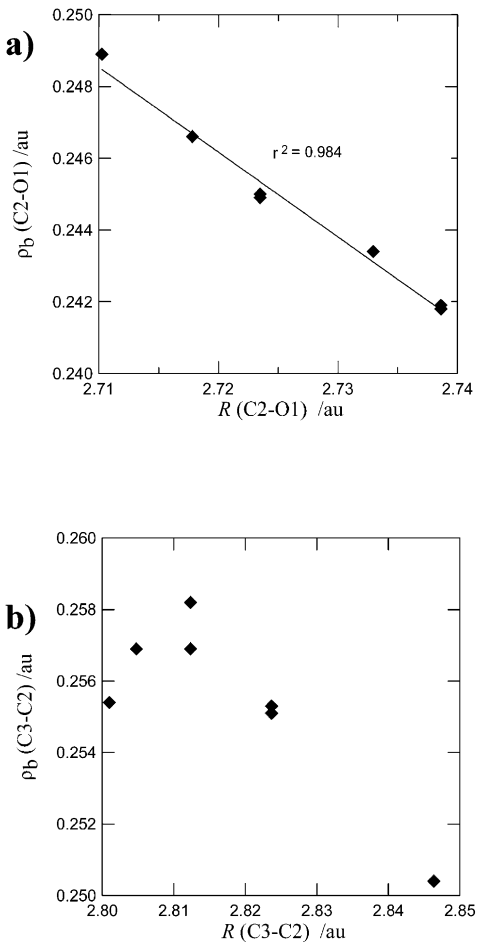

Fig. 2. Plot of the charge density at the critical points vs. the length of the bond path; (a)C2–O1 bond, (b)C3–C2 bond.

(Fig. 1). The (a) conformer (with the H^+ introduced at the opposite side that the majority of the methyl substituents) was found to be slightly more stable than (b).

The geometrical parameters of the C_2–O_1–C_3 ring structure have been shown in Table 2, which also displays the difference between the earlier defined AIL length and the geometrical distance between the nuclei, Δl_{IJ}. The corresponding difference for the C–O–C bond angle, $\Delta\alpha$, is also listed in Table 2. According to our literature search, there is only experimentally measured structure for oxirane [30] ($r_{C\text{–}C} = 1.466$ Å, $r_{C\text{–}O} = 1.431$ Å). The B3LYP/6-311++G(d,p) bond lengths (Table 2) agree with these values within 0.001 Å. The experimental C–H bond distance (1.085 Å) is also quite close to the calculated value (1.087 Å).

Methyl-substitution leads to a dispersion of the ring electron density over more H atoms [23], thereby leading to a lengthening of ring peripheral bonds. As methyl replaces hydrogen, the charge density at the BCP decreases in the C–O bonds, on the other hand the variations of the charge at the C–C BCP are not keeping in line with this interpretation (Table 3, Fig. 2). Linear correlations between the charge density at BCP and bond length have been previously established for covalent [31] and hydrogen bonds [32,33]. Also, a logarithmic relationship, allowing the simultaneous treatment of C–H covalent bondlengths and hydrogen bond C···H distances has been reported [34]. ρ_b vs. R linear correlations (Fig. 2(a)) were found to be reasonable for the C–O bonds in this series, but too rough to be useful for the cyclic C–C bonds (Fig. 2(b)).

The unusual relationship between ρ_b and R for the C–C bond could be attributed to the fact that the charge density is concentrated to an appreciable extent over the entire surface of the ring in three membered ring (3MR) compounds. Thus, the ratio, η, between the charge density at the RCP, ρ_r, and the average of the charge density at the three peripheral BCPs is larger than 0.83 (Table 4). This ratio serves as a measure of the σ-electron density surface delocalisation [3]. Its value indicates that charge density is highly delocalised in this compound. The position of the ring critical point, that is substantially closer to the C–C BCP than to the C–O BCPs (Table 4), indicates that the charge in the C–C bond region is markedly affected by the charge delocalised over the ring, and, therefore, it is plausible that ρ_b fails to correlate with the C–C bond distance.

There exists a good linear correlation between the electron surface delocalisation index η and the number of methyl groups attached to the carbons forming the ring. The same holds for the summation of the peripheral bond lengths as can be seen in Fig. 3.

The value of $\nabla^2\rho_b$ parallels ρ_b in its behaviour, becoming slightly less negative as the charge density at the BCP decreases upon methyl substitution (Table 3). The C–O and C–C bonds of the ring have substantial ellipticities, reflecting the electron density delocalisation over the surface of the ring. The rate of fall off experienced, at the ring peripheral BCPs, by the

Table 4
Local properties at the C–O–C ring critical point; distances (R_i) from the ring critical point to atom i and distances (R_{i-j}) from the ring critical point to the bond critical point associated to the atoms i and j. All data, except η, in au

Complex	ρ_r	$\nabla^2\rho_r$	$\eta\cdot100$	R_{O1}	R_{C2}	R_{C3}	R_{O1-C2}	R_{O1-C3}	R_{C2-C3}
1	0.2092	0.3134	83.3	1.70	1.52	1.52	0.914	0.915	0.765
2	0.2079	0.3235	83.1	1.70	1.52	1.53	0.907	0.912	0.780
3	0.2063	0.3307	82.8	1.70	1.54	1.52	0.894	0.923	0.789
4	0.2065	0.3332	82.8	1.70	1.53	1.53	0.906	0.906	0.793
5	0.2054	0.3333	82.7	1.70	1.53	1.53	0.913	0.914	0.786
6	0.2036	0.3404	82.3	1.70	1.54	1.53	0.901	0.924	0.795
7	0.2002	0.3472	81.8	1.71	1.54	1.54	0.924	0.925	0.794
1 +	0.1784	0.3597	81.9	1.71	1.61	1.61	0.689	0.688	0.963
2 + (b)	0.1689	0.3193	79.1	1.72	1.47	1.83	0.239	1.021	1.054
4 +	0.1655	0.3699	79.0	1.72	1.63	1.67	0.624	0.720	1.024
5 + (a)	0.1652	0.3683	79.6	1.73	1.65	1.65	0.681	0.680	1.233
5 + (b)	0.1663	0.3669	79.8	1.73	1.65	1.65	0.686	0.686	1.018
7 +	0.1552	0.3713	77.9	1.74	1.69	1.69	0.692	0.695	1.056

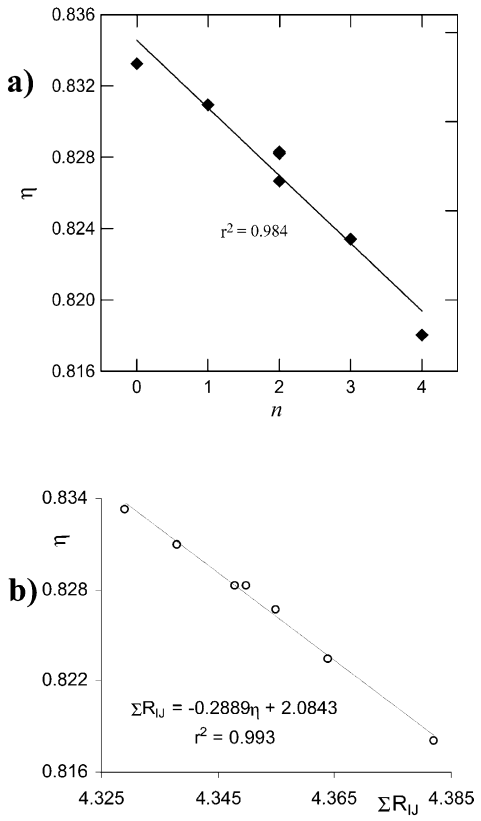

Fig. 3. Linear correlation between the estimation of electron density surface delocalisation (η) and: (a) the number of methyl groups (n) attached to the ring; (b) the summation of the ring peripheral bond distances. See text for further details.

charge density is lower in any direction that is parallel to the surface of the ring than in the perpendicular direction (i.e. in oxirane the values of the two negative curvatures are −0.460 and −0.284 a.u., respectively). The ellipticity of the C–O bond in methoxymethane is calculated to be approximately one order of magnitude less than that of oxirane at the same computational level.

All the AILs defining the 3MR oxirane structure are found to be outwardly curved (Fig. 4). The C–O AIL differs slightly from the internuclear line, whereas both lines are substantially different for the C–C bond, yielding significant Δl_{23} values (Table 2) that surpass those for cyclopropane at the same computational level (1.514 Å for the AIL and 1.508 Å for the bond length). The difference between the COC angle and that formed by both C–O AIL ranges from 11.6 to 12.7° upon methylation. This difference is about the same for the OCC angles (ranging from 11.3° in **1** to 13.0° in **7**). Differences for both OCC and COC angles are smaller in oxiranes than for CCC angles in cyclopropane (15.3°).

The protonation process for **2a** + , that results in the 3MR opening is, like any other ring opening [35], an example of bifurcation catastrophe (Fig. 5). The transition state for the process has an unstable gradient vector field characterised by the coalescence of the RCP and the C–O BCP into a degenerated critical point, where one of the curvatures perpendicular to the C–O bond vanishes. Even when the cycle is not opened, protonation leads to noticeable variations in

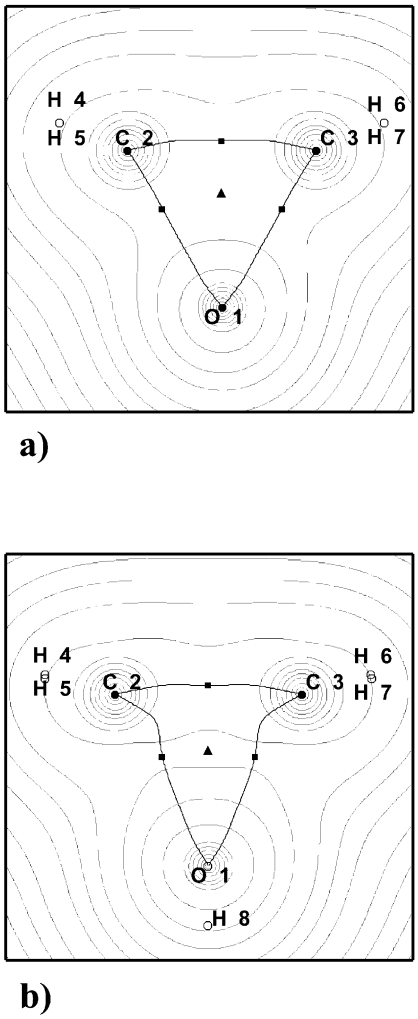

Fig. 4. Superposition of the contour lines (thin) of the charge density with the molecular graphs (bold) in (a) oxirane and (b) protonated oxirane. Nuclei are represented by (●) and the symbols (■) and (▲) represent the locations of bond and ring critical points, respectively. Projections of out-of-plane atoms are represented by (○).

the geometrical parameters of the COC ring. The greatest variations involve the parameters related to the oxygen atom. Thus, C–O bonds are more labile than the C–C bond, which remains nearly unperturbed. As a consequence COC angle is closed by 5–6° (Table 2). The AIL structure also changes by protonation from an outwardly curved to a partially inwardly curved triangle (Fig. 4) keeping an outward bent C–C AIL, as it was previously found and discussed by Cremer and Kraka at the HF level [3].

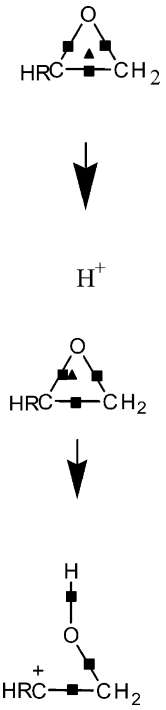

Fig. 5. Scheme showing the variation of ring and bond critical points along the 2 + (a) protonation process. The symbols (■) and (▲) represent the locations of bond and ring critical points, respectively.

It it also important to note that several C–O bonds in the protonated forms present positive $\nabla^2\rho_b$ values. Though $\nabla^2\rho_b$ provides a measure of the extent to which the charge density is locally depleted or concentrated from a given point [21,22], positive values of $\nabla^2\rho_b$ have been found in the whole bound region for bonds between strongly electronegative atoms [24]. Thus, $\nabla^2\rho_b$ values for the C=O bond of carbonyl compounds [3,36] were found to be positive. Also, $\nabla^2\rho_b$ positive values have been calculated for C ≡ N bonds [37] and BCPs within diffuse charge distribution regions [38]. In this case, the $\nabla^2\rho_b$ positive value can be explained in terms of the proximity of the BCP to one of the nodes in the valence shell charge concentration (VSCC). Because of the inwardly shape of the AIL in protonated oxiranes, the BCP is located inside the local charge depletion area occupying the centre of the ring (this is found at both the B3LYP and HF [3] computational levels). The negative computed value for the total energy density function, H_b, in the C–O bonds (Table 3) corresponds to a covalent bond interaction [3,24].

Table 5
H–H distances (Å) and electron density local properties (au) at C–H···H–C bond critical points. See text for further details

Comp	Interaction	R_{H-H}	Δl	$10^3\rho_b$	$\nabla^2\rho_b$	10^3H_b	ε	$10^3\rho_r$	$\nabla^2\rho_r$	R_{b-r}
5	H_{12}–H_{10}	2.183	0.411	9.1	0.0327	1.6	1.443	8.9	0.0385	0.436
5[a]	H_{12}–H_{10}	2.206	0.520	8.8	0.0354	2.2	1.982	8.8	0.0375	0.364
5[b]	H_{12}–H_{10}	2.107	0.396	10.6	0.0384	1.8	1.390	10.4	0.0446	0.471
6	H_{15}–H_9	2.137	0.378	9.9	0.0353	1.7	1.090	9.6	0.0426	0.609
7	H_{16}–H_{12}, H_{18}–H_{10}	2.019	0.307	12.3	0.0434	2.0	0.651	11.3	0.0534	0.797

[a] Local properties from HF/6-311++G(d,p) electron distributions.
[b] Local properties from MP2/6-311++G(d,p) electron distributions.

3.1. Unusual H···H interactions

At this point, it has to be stressed that the usual chemical Lewis structure does not always reflect all the atom–atom interactions within a given molecule. In fact, in this work C–H···H–C AILs have been located in several methyl-substituted oxiranes (**5**, **6**, and **7**, Table 5) and their protonated forms. Fig. 6 shows the two interacting hydrogens in *cis* 1,2-dimethyl oxirane (**5**). This result has also been confirmed at other computational levels (namely, HF/6-311++G(d,p) and MP2/6-311++G(d,p)), in order to reject possible artefacts from our calculations. The quantitative changes upon replacing the present wave function by the earlier-mentioned ones were found to be relatively small, as shown in Table 5 for the H···H contacts in *cis* 1,2-dimethyl oxirane. Hydrogen bonds where the donor atom is also a hydrogen (dihydrogen bonds) have been described in the chemical literature [39–41], and characterised by using the AIM theory [42–45]. However, to the best of our knowledge all the dihydrogen bonds hitherto described connect hydrogens linked to atoms with a very different electronegativity. This is not the case, even in molecules **5** and **7** the hydrogens connected are related by a reflection in a plane of symmetry. The presence of AILs between the hydrogens connected to 1,4-carbon atoms in similar symmetrical environments was associated with non-bonding repulsive interactions [46], though this association was criticised in a later work [47].

Due to the existence of these unexpected BCPs, the theorem of Poincaré-Hopf [48] demands the existence of a new RCP. This point is located significantly far from the BCP (Table 5). The charge density at the bond (ρ_b), and ring critical point (ρ_r) are very similar, and one order of magnitude lower than those calculated for covalent bonds. The corresponding Laplacians of the charge density are small in magnitude and positive, indicating that the charge density is not accumulated in these points, but concentrated towards the atomic basins. The positive H_b values are in line with this interpretation, pointing to the association of these AILs with closed-shell interactions [49]. As

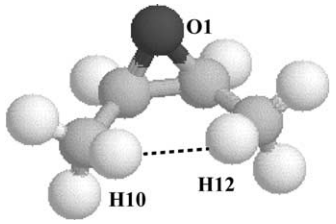

Fig. 6. C–H···H–C AIL in *cis* 1,2-dimethyl oxirane (**5**).

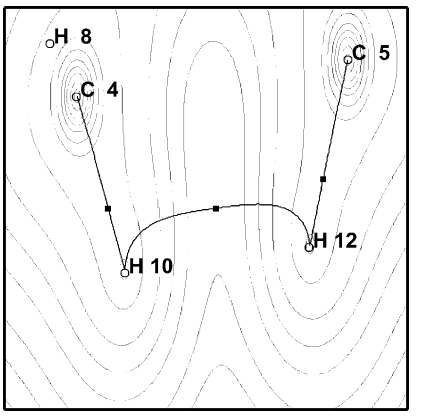

Fig. 7. Superposition of the contour lines (thin) of the charge density in the C–H···H–C AIL area with the molecular graphs (bold) in *cis* 1,2-dimethyl oxirane (**5**). Nuclei are represented by (●) and the symbol (■) represents the locations of bond critical points.

Table 6
Atomic and bond properties for the oxygen fragment in the alkyl-substituted oxiranes studied herein. All values are given in au (note: − and + represent bond properties referring to the bond critical point between the oxygen and carbon atoms C2 and C3, respectively)

Group	R1	R2	R3	R4	N(O)	$-E$(O)	$10^2\mu$(O)	ν(O)	10^4L(O)	ρ_b^-	ρ_b^+	R_b^-	R_b^+
A	H	H	H	H	8.895	75.7378	0.4	94.9	0.2	0.2489	0.2489	1.705	1.705
B	Me	H	H	H	8.899	75.7604	1.4	94.5	−1.2	0.2466	0.2471	1.707	1.707
C	Et	H	H	H	8.901	75.7749	1.0	94.6	0.1	0.2469	0.2469	1.708	1.708
	Pr	H	H	H	8.901	75.7835	1.0	94.4	1.0	0.2465	0.2465	1.707	1.704
D	Me	H	H	Me	8.905	75.7755	2.4	94.7	0.3	0.2449	0.2449	1.705	1.705
	Me	H	Me	H	8.906	75.7774	2.4	94.6	1.6	0.2450	0.2451	1.706	1.706
E	Et	H	H	Me	8.907	75.7858	2.0	94.6	0.3	0.2452	0.2448	1.706	1.705
	Pr	H	H	Me	8.906	75.7918	2.1	94.5	0.3	0.2448	0.2449	1.706	1.705
F	Et	H	H	Et	8.908	75.7904	2.2	95.0	0.6	0.2453	0.2448	1.706	1.706
	Pr	H	H	Et	8.907	75.7949	2.2	95.1	0.3	0.2449	0.2435	1.706	1.707
	Pr	H	H	Pr	8.907	75.7991	2.2	95.0	2.5	0.2451	0.2410	1.707	1.707
G	Me	Me	H	H	8.902	75.7753	2.7	94.2	2.3	0.2434	0.2469	1.707	1.702
H	Me	Me	Me	H	8.909	75.7877	3.5	94.3	0.4	0.2418	0.2449	1.706	1.704
J	Me	Me	Me	Me	8.913	75.7971	4.2	93.9	1.5	0.2419	0.2419	1.705	1.705

shown in Fig. 7, the AIL connecting the two interacting hydrogens deviates substantially from the internuclear line as was previously observed in other systems [46]. Correspondingly, Δl values are large, if compared with those in the C–C bonds (Table 2). The increasing of H···H distance leads to a diminution of the distance between the ring critical point and increased AIL lengths. As was previously pointed out, the H–H distance is the variable controlling the presence of such H···H contacts [46], though the H···H contact here calculated for **5** at the HF level exceeds the limiting value of 2.18 Å proposed in that work. Topological properties for other BCPs have not been reported in the interest of space, as no other unusual bond paths or properties were found.

4. Approximate transferability of the oxygen atom

The non-energetic values of the main atomic and bond properties of the oxygen atom in the series of the 14 oxiranes here studied can be grouped into approximately transferable values by distinguishing a total of nine different molecular environments (A to J in Table 6). In order to describe these environments it is useful to consider a related open chain ether for every oxirane. This related compound is, for every molecule, the result of a hypothetical hydrogenation of the C–C bond in the cycle. Thus, the 14 oxiranes here studied can be classified into two series: (a) compounds related to linear unbranched ethers (hereafter indicated by the acronym CRLUE): **1**, **2**, **4**, **5**, **8**–**14**; and (b) compounds related to branched dialkylethers (hereafter indicated by the acronym CRLBE): **3**, **6** and **7**.

It is remarkable that, though absolute values are substantially different from those of oxygen in linear dialkylethers, their evolution along the CRLUE series can be interpreted by employing the same classification that was previously proposed for dialkylethers [17]. The highly specific nature of oxygen in parent oxirane, **1**, (environment A) is reminiscent of the methoxymethane in dialkylethers. There is also an important difference between the properties exhibited by the oxygen atom in monosubstituted (B, and C) and disubstituted oxiranes (C, D, and E). The gap observed in the values of the properties between monomethyl, 1,2-dimethyloxiranes and the remaining mono or disubstituted oxiranes is approximately equivalent to that found between methylethers and the remaining dialkylethers at the HF level [17]. On the other hand, the size of the substituent origins a slight difference between the oxygen of the oxiranes if we replace one or two methyl with longer substituents, yielding negligible consequences on the atomic and bond properties of the oxygen atom when ethyl is replaced by longer substituents. CRBLE oxiranes **3**, **6**, and **7** display very different values for the majority of the quantities presented in Table 6.

5. Conclusions

The DFT calculations presented here were satisfactory in reproducing the available geometrical parameters. The data and discussion in previous sections, lead us to the following major conclusions:

1. The COC ring structure remains quite rigid upon the replacement of hydrogens by methyl groups. The RCP (at which the charge density is still more than 80% of the average charge density at the ring peripheral BCPs) is closer to the C–C BCP than to the C–O BCPs, resulting in a rough correlation between the C–C bond distance and the charge density at the corresponding BCP.
2. Oxygen protonation of several oxiranes with methyl susbstituents results in ring opening through a bifurcation catastrophe, in which the RCP and the C–O BCP merge into a degenerated critical point. The total energy density function confirms the covalent character of C–O bonds in the protonated forms possessing positive $\nabla^2\rho_b$ values.
3. The topology of the electron density of several methylated oxiranes and their protonated forms shows the existence of closed-shell interaction between hydrogen atoms attached to carbon atoms in 1,4-positions.
4. Regarding the transferability of non-energetic atomic and bond properties, oxygen atoms in alkyl-substituted oxiranes can be classified into two groups according to the homologous linear (branched or unbranched) monoether that would be produced by the hypothetical hydrogenation of the C–C cyclic bond. Their evolution within each series can be rationalised by considering the same six groups previously described in linear unbranched ethers.

Acknowledgements

Financial support from Xunta de Galicia and generous computational resources provided by Centro de Supercomputación de Galicia are acknowledged. We are also indebted to Estela and Alba Surís for fruitful comments on this manuscript.

References

[1] L.A. Paquette (Ed.), Handbook of Reagents for Organic Synthesis Wiley, Chichester, 1999.
[2] A. Vila, R.A. Mosquera, Tetrahedron 57 (2001) 9415.
[3] D. Cremer, E. Kraka, J. Am. Chem. Soc. 107 (1985) 3800.
[4] S.M. Bachrach, A. Streitweiser, J. Comput. Chem. 10 (1989) 514.
[5] J.A. Boatz, M. Gordon, J. Phys. Chem. 93 (1989) 3025.
[6] C. Lian, L.C. Allen, J. Am. Chem. Soc. 113 (1991) 1878.
[7] P.K. Bose, T.M. Black, P.L. Polavarapu, Chem. Phys. 139 (1989) 409.
[8] M. Alcamí, O. Mó, M. Yáñez, J. Comput. Chem. 19 (1998) 1072.
[9] P. George, C.W. Bock, J.P. Glusker, J. Phys. Chem. 96 (1992) 3702.
[10] J. Catalán, M. Yáñez, J. Am. Chem. Soc. 100 (1978) 1398.
[11] O. Mó, J.L.G. De Paz, M. Yáñez, J. Phys. Chem. 91 (1987) 6484.
[12] D.H. Aue, H.M. Webb, W.R. Davidson, M. Vidal, M.T. Bowers, H. Goldwhite, L.E. Vertal, J.E. Douglas, P.A. Kollman, G.L. Kenyon, J. Am. Chem. Soc. 102 (1980) 5151.
[13] C. Bock, P. George, J.P. Glusker, J. Org. Chem. 58 (1993) 5816.
[14] J.M. Coxon, R.G.A.R. Maclagan, A. Rauk, A.J. Thorpe, D. Whalen, J. Am. Chem. Soc. 119 (1997) 4712.
[15] R.H. Nobes, W.R. Rodwell, W.J. Bouma, L. Radom, J. Am. Chem. Soc. 103 (1981) 1913.
[16] J.J. BelBruno, Chem. Phys. Lett. 263 (1986) 84.
[17] A. Vila, E. Carballo, R.A. Mosquera, Can. J. Chem. 78 (2000) 1535.
[18] A. Vila, R.A. Mosquera, J. Chem. Phys. 115 (2001) 1264.
[19] A. Vila, R.A. Mosquera, Chem. Phys. Lett. 345 (2001) 445.
[20] A. Vila, R.A. Mosquera, Chem. Phys. Lett. 332 (2000) 474.
[21] R.F.W. Bader, Atoms in Molecules, A Quantum Theory, International Series of Monographs in Chemistry, vol. 22, Oxford University Press, Oxford, 1990.
[22] R.F.W. Bader, Chem. Rev. 91 (1991) 893.
[23] A. Vila, R.A. Mosquera, submitted for publication.
[24] D. Cremer, E. Kraka, Angew. Chem., Int. Ed. Engl. 23 (1984) 627.
[25] M.J. Frisch, G.W. Trucks, H.B. Schlegel, P.M.W. Gill, B.G. Johnson, M.A. Robb, J.R. Cheeseman, T. Keith, G.A. Petersson, J.A. Montgomery, K. Raghavachari, M.A. Al-Laham, V.G. Zakrzewski, J.V. Ortiz, J.B. Foresman, J. Cioslowski, B.B. Stefanov, A. Nanayakkara, M. Challacombe, C.Y. Peng, P.Y. Ayala, W. Chen, M.W. Wong, J.L. Andres, E.S. Replogle, R. Gomperts, R.L. Martin, D.J. Fox, S. Binkley, D.J. Defrees, J. Baker, J.P. Stewart, M. Head-Gordon, C. Gonzalez, J.A. Pople, GAUSSIAN 94, Revision C.3, Gaussian, Inc., Pittsburgh PA, 1995.
[26] MORPHY98, a topological analysis program written by P.L.A. Popelier with a contribution from R.G.A. Bone (UMIST, Engl., EU).
[27] P.L.A. Popelier, Chem. Phys. Lett. 288 (1994) 160.
[28] F.W. Biegler-Koenig, R.F.W. Bader, T.-H. Tang, J. Comput. Chem. 3 (1982) 317.

[29] AIMPAC: a suite of programs for the theory of atoms in molecules, in: R.F.W. Bader et al. (Eds.), McMaster University, Hamilton, Ont., Canada, L8S 4M1. Contact bader@mcmail.cis.mcmaster ca.
[30] G.L. Cunningham, A.W. Boyd, R.J. Myers, W.D. Gwinn, J. Chem. Phys. 19 (1951) 676.
[31] K.B. Wiberg, C.M. Breneman, J. Am. Chem. Soc. 112 (1990) 8765.
[32] R.J. Boyd, S.C. Choi, Chem. Phys. Lett. 120 (1985) 80.
[33] R.J. Boyd, S.C. Choi, Chem. Phys. Lett. 129 (1986) 62.
[34] I. Alkorta, I. Rozas, J. Elguero, Struct. Chem. 9 (1998) 243.
[35] R.F.W. Bader, Y. Tal, S.G. Anderson, T.T. Nguyen-Dang, Isr. J. Chem. 19 (1980) 8.
[36] A.M. Graña, R.A. Mosquera, J. Chem. Phys. 110 (1999) 6606.
[37] T.-S. Hwang, Y. Wang, J. Phys. Chem. A 102 (1998) 3726.
[38] G.T. Smith, P.R. Mallinson, C.S. Frampton, L.J. Farrugia, R.D. Peacock, J.A.K. Howard, J. Am. Chem. Soc. 119 (1997) 5028.
[39] T.B. Richardson, S. De Gala, R.H. Crabtree, P.E.M. Siegbahn, J. Am. Chem. Soc. 117 (1995) 12875.
[40] R.H. Crabtree, P.E.M. Siegbahn, O. Eisenstein, A.L. Rheingold, T.F. Koetzle, Acc. Chem. Res. 29 (1996) 348.
[41] M. Remko, Mol. Phys. 94 (1998) 839.
[42] S.A. Kulkarni, J. Phys. Chem. A 102 (1998) 7704.
[43] S.A. Kulkarni, A.K. Srivastava, J. Phys. Chem. A 103 (1999) 2836.
[44] S.A. Kulkarni, J. Phys. Chem. A 103 (1999) 9330.
[45] P.L.A. Popelier, J. Phys. Chem. A 102 (1998) 1873.
[46] J. Cioslowski, S.T. Mixon, Can. J. Chem. 70 (1992) 443.
[47] R.F.W. Bader, J. Phys. Chem. A 102 (1998) 7314.
[48] K. Collard, G.G. Hall, Int. J. Quantum Chem. 12 (1977) 623.
[49] R.G.A. Bone, R.F.W. Bader, J. Phys. Chem. 100 (1996) 10892.